Cancer Cell
Article

Endothelial CCR2 Signaling Induced by Colon Carcinoma Cells Enables Extravasation via the JAK2-Stat5 and p38MAPK Pathway

Monika Julia Wolf,[1,12] Alexandra Hoos,[4,12] Judith Bauer,[5] Steffen Boettcher,[2] Markus Knust,[6,7] Achim Weber,[3] Nicole Simonavicius,[5] Christoph Schneider,[8] Matthias Lang,[6] Michael Stürzl,[9] Roland S. Croner,[9] Andreas Konrad,[9] Markus G. Manz,[2] Holger Moch,[3] Adriano Aguzzi,[1] Geert van Loo,[10] Manolis Pasparakis,[11] Marco Prinz,[6] Lubor Borsig,[4,13,*] and Mathias Heikenwalder[1,5,13,*]

[1]Institute of Neuropathology
[2]Division of Hematology
[3]Institute of Surgical Pathology
University Hospital Zurich, CH-8091 Zurich, Switzerland
[4]Institute of Physiology, Zurich Center for Integrative Human Physiology, University of Zurich, CH-8057 Zurich, Switzerland
[5]Institute of Virology, Technische Universität München/Helmholtz Zentrum München, D-81675 Munich, Germany
[6]Department of Neuropathology & BIOSS Centre for Biological Signaling Studies, University of Freiburg, D-79106 Freiburg, Germany
[7]Faculty of Biology, University of Freiburg, D-79104 Freiburg, Germany
[8]Institute of Integrative Biology, ETH Zurich, CH-8952 Schlieren, Switzerland
[9]Division of Molecular and Experimental Surgery, Department of Surgery, University Hospital Erlangen, D-91054 Erlangen, Germany
[10]Department for Molecular Biomedical Research, VIB Gent, B-9052 Gent-Zwijnaarde, Belgium
[11]Institute of Genetics, Centre for Molecular Medicine (CMMC) and Cologne Excellence Cluster on Cellular Stress Responses in Aging-Associated Diseases (CECAD), University of Cologne, D-50674 Cologne, Germany
[12]These authors contributed equally to this work
[13]These authors contributed equally to this work
*Correspondence: lborsig@access.uzh.ch (L.B.), heikenwaelder@helmholtz-muenchen.de (M.H.)
http://dx.doi.org/10.1016/j.ccr.2012.05.023

SUMMARY

Increased expression of the chemokine CCL2 in tumor cells correlates with enhanced metastasis, poor prognosis, and recruitment of CCR2^{+}Ly6C^{hi} monocytes. However, the mechanisms driving tumor cell extravasation through the endothelium remain elusive. Here, we describe CCL2 upregulation in metastatic UICC stage IV colon carcinomas and demonstrate that tumor cell-derived CCL2 activates the CCR2^{+} endothelium to increase vascular permeability in vivo. CCR2 deficiency prevents colon carcinoma extravasation and metastasis. Of note, CCR2 expression on radio-resistant cells or endothelial CCR2 expression restores extravasation and metastasis in *Ccr2*$^{-/-}$ mice. Reduction of CCR2 expression on myeloid cells decreases but does not prevent metastasis. CCL2-induced vascular permeability and metastasis is dependent on JAK2-Stat5 and p38MAPK signaling. Our study identifies potential targets for treating CCL2-dependent metastasis.

INTRODUCTION

Metastasis, the spread of tumor cells to vital organs, is the leading cause of cancer-related death in humans (Gupta and Massagué, 2006). Understanding the mechanisms driving metastasis is therefore essential for developing new therapeutic strategies. Metastasis is a multistage process comprising tumor cell dissemination, survival in the circulation, extravasation, and ultimately colonization of distant organs (Chambers et al., 2002; Joyce and Pollard, 2009). Tumor cell extravasation, colonization

Significance

Metastasis is the primary cause of cancer-related mortality. Elevated expression of CCL2 attracts CCR2^{+}Ly6C^{hi} monocytes and enhances metastasis. We show that metastatic UICC stage IV colon carcinomas upregulate CCL2. Using both in vivo and in vitro models, we demonstrate that colon carcinoma-derived CCL2 activates endothelial cells through CCR2 and is dependent on JAK2-Stat5 and p38MAPK phosphorylation. Our results show that a tumor cell-derived chemokine induces vascular permeability and enables efficient tumor cell extravasation, suggesting a so-far undescribed role for chemokines in tumor cell extravasation. Moreover, we identified two targets for the suppression of CCL2-dependent tumor cell extravasation during colon carcinoma metastasis. Chemokine-dependent control of vascular permeability during metastasis is likely to occur in various cancers.

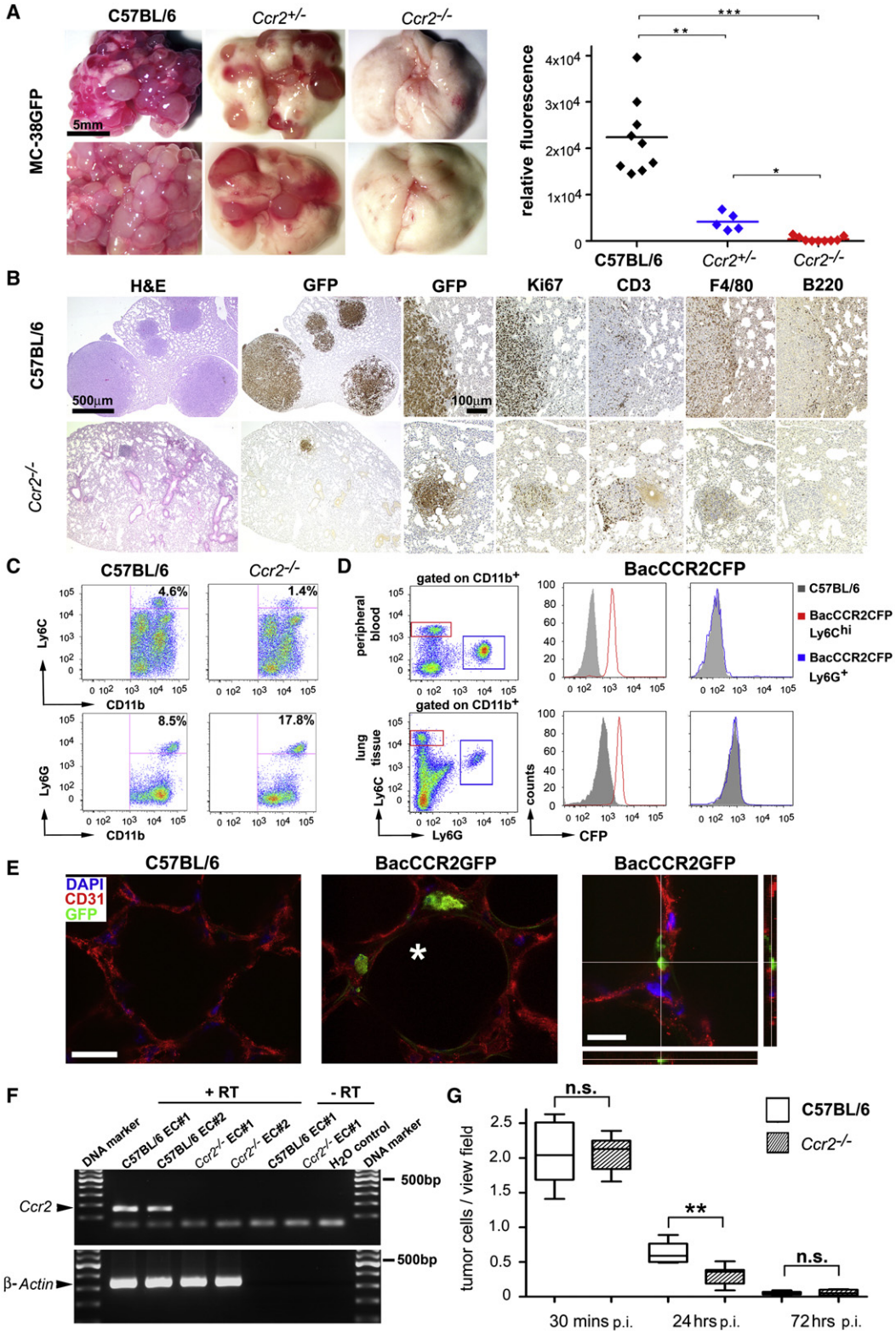

Figure 1. CCR2 Determines Susceptibility to Experimental Lung Metastasis in a Dose-Dependent Manner

(A) Macroscopy of lungs derived from C57BL/6 (n = 9), *Ccr2*$^{+/-}$ (n = 5), *Ccr2*$^{-/-}$ mice (n = 9) on day 28 p.i. with MC-38GFP cells. Size of scale bar is indicated (left panel). Quantification of tumor load by GFP fluorescence in lung homogenates (right panel).

(B) Histological analysis of colon carcinoma tumors (MC-38GFP) in C57BL/6 and *Ccr2*$^{-/-}$ lungs at 28 d.p.i. Low and high magnifications (scale bars) are indicated. H&E, hematoxylin and eosin; GFP, tumor cells; Ki67, proliferating cells; CD3, T cells; F4/80, macrophages, B220: B cells.

as well as outgrowth are considered to be the limiting steps in metastasis (Chambers et al., 2002). It has long been recognized that the tumor cell microenvironment, composed of fibroblasts, endothelial cells, and leukocytes, significantly contributes to metastatic dissemination (Joyce and Pollard, 2009). In particular, myeloid-derived monocytes/macrophages, commonly found in various types of malignant cancers were shown to facilitate tumor cell extravasation and metastatic outgrowth (Peinado et al., 2011; Qian and Pollard, 2010). Analysis of the metastasis-supporting niche revealed that soluble factors derived from the local environment and from tumors are responsible for mobilization of bone marrow (BM)-derived cells during metastasis (Peinado et al., 2011).

Chemokines and their receptors were found to be involved in metastasis and also to be direct targets of oncogene activation (Allavena et al., 2011; Hiratsuka et al., 2006). Stromal cells, infiltrating leukocytes and tumor cells themselves were identified as sources of cytokines and chemokines, both at primary tumors and metastatic sites (Läubli and Borsig, 2010; Mishra et al., 2011; O'Hayre et al., 2008). Highly metastatic cells have been shown to induce BM-derived macrophages to express cytokines and chemokines emphasizing the role of a reciprocal crosstalk of tumor cells with the microenvironment to actively shape the metastatic niche (Kim et al., 2009). Local activation of endothelia by metastasizing tumor cells induced CCL5 expression, which was associated with monocyte recruitment during the initial phase of metastasis. Accordingly, inhibition of CCL5 reduced metastasis (Läubli et al., 2009). Recently, CCL2 has been identified as the major factor facilitating breast cancer metastasis to the lung (Qian et al., 2011). Clinical evidence clearly associated elevated levels of CCL2 and CCL5 with poor prognosis in breast, colon, prostate, and cervix cancer patients due to metastatic progression (Soria et al., 2011; Yoshidome et al., 2009; Zhang et al., 2010; Zijlmans et al., 2006). Monocytes recruited to tumors through the CCL2-CCR2 axis can be polarized to an alternatively activated M2-phenotype thereby contributing to immunosuppression and enhanced tumor cell survival (Loberg et al., 2007; Mantovani and Sica, 2010). CCL2 has been shown to induce angiogenic activation of endothelial cells along with inflammatory responses (Salcedo et al., 2000), and CCL2-mediated recruitment of inflammatory monocytes promoted metastasis (Qian et al., 2011). Similarly, overexpression of CCL2 in PC-3 prostate cancer cells led to increased bone metastasis associated with elevated accumulation of macrophages (Mizutani et al., 2009). Consequently, CCL2-neutralizing antibody treatment significantly prolonged survival of tumor-bearing mice due to inhibition of metastasis (Lu and Kang, 2009; Mizutani et al., 2009; Qian et al., 2011; Salcedo et al., 2000). Although elevated CCL2 expression is clearly linked to metastasis through the recruitment of monocytes/macrophages, the exact mechanisms by which CCL2 signaling facilitates tumor cell extravasation at the endothelial barrier and subsequent metastatic colonization remain elusive.

Here, we investigate the role of the CCL2-CCR2 chemokine axis during metastatic dissemination and the involvement of the endothelium in this process.

RESULTS

CCR2 Promotes Metastasis of Colon Carcinoma Cells

To determine whether tumor cell extravasation and growth was altered in the absence of CCR2, C57BL/6 and *Ccr2*$^{-/-}$ mice were intravenously (i.v.) injected with syngeneic GFP^{+} colon carcinoma cells (MC-38GFP) and lungs were macroscopically scored for the presence of metastatic foci 28 days postinjection (d.p.i.). *Ccr2*$^{-/-}$ lungs displayed fewer tumors than C57BL/6 lungs ($p < 0.001$; Figure 1A; Figure S1A available online). Development of tumors depended on CCR2 expression levels in the recipient host, since *Ccr2*$^{+/-}$ lungs contained fewer metastases than C57BL/6 ($p < 0.01$) but still more than *Ccr2*$^{-/-}$ ($p < 0.05$; Figures 1A, S1A, and S1B). This was corroborated by measurement of relative GFP fluorescence in lung homogenates (Figure 1A). Immunohistochemistry revealed no obvious differences in the relative composition of Ki67^{+}, CD3^{+}, F4/80^{+}, and B220^{+} cells within the tumors (Figure 1B).

Next, we investigated whether differences in the immune cell composition could influence metastasis. No differences in numbers of CD4^{+} or CD8^{+} T cells, CD19^{+} B cells, NK1.1^{+}, or F4/80^{+} cells could be identified between naive C57BL/6 and *Ccr2*$^{-/-}$ lungs by flow cytometry (Figure S1C). However, *Ccr2*$^{-/-}$ lungs displayed reduced numbers of CD11b^{+}Ly6C^{hi}Ly6G^{-} monocytes ($p < 0.001$; denoted as Ly6C^{hi}) and a relative increase in CD11b^{+}Ly6G^{+} cells ($p < 0.01$; Figures 1C, S1D, and S1E). To identify which cells express CCR2, we performed flow cytometry on blood and lung tissue from BacCCR2CFP reporter mice, expressing CFP under the CCR2 promoter (Hohl et al., 2009). Almost all CD11b^{+}Ly6C^{hi} cells were CFP positive, whereas CD11b^{+}Ly6G^{+}, CD19^{+}, CD4^{+}, and CD8^{+} cells were CFP negative (Figures 1D and S1F). We next investigated whether nonhematopoietic cells in lungs express CCR2. Confocal microscopy of BacCCR2GFP mice revealed that CD31^{+} lung endothelial cells expressed GFP (Figures 1E and S1G), as confirmed by transcriptional analysis of purified primary endothelial cells from C57BL/6 and *Ccr2*$^{-/-}$ lungs (Figures 1F, S1I, and S1J).

Altered numbers of colon carcinoma cells in lungs of *Ccr2*$^{-/-}$ mice could explain the observed inability to form tumors. However, no differences in the amount and distribution of

(C) Flow cytometry analysis of monocytes in naive lungs of *Ccr2*$^{-/-}$ and C57BL/6 mice.
(D) Flow cytometry of CFP^{+} cells in blood and lung tissue of BacCCR2CFP transgenic mice shows that most Ly6C^{hi} (red) but no Ly6G (blue) cells express CFP.
(E) Confocal microscopy analysis on lung tissue of C57BL/6 and BacCCR2GFP mice for the expression of GFP. Endothelial cells are positive for GFP (green) and CD31 (red); nuclei are stained in blue (DAPI). The asterisk indicates the alveolar space; scale bars: 20 μm (low magnification); 15 μm (high magnification); Z-stacks are indicated.
(F) RT-PCR of *Ccr2* expression in CD31-sorted primary endothelial cells isolated from lungs of C57BL/6 and *Ccr2*$^{-/-}$ mice. Two samples for each genotype are shown (+RT), including controls without reverse transcriptase treatment (-RT). *β-actin* served as control (bp, base pairs).
(G) Time course analysis of tumor cell survival in lung tissue. Numbers of tumor cells/view field were analyzed on sections of C57BL/6 and *Ccr2*$^{-/-}$ lungs 30 min, 24 hr and 72 hr p.i. (n = 3, each; mean with min/max is shown). Statistics: ***$p < 0.001$; **$p < 0.01$; *$p < 0.05$; n.s., not significant.
See also Figure S1.

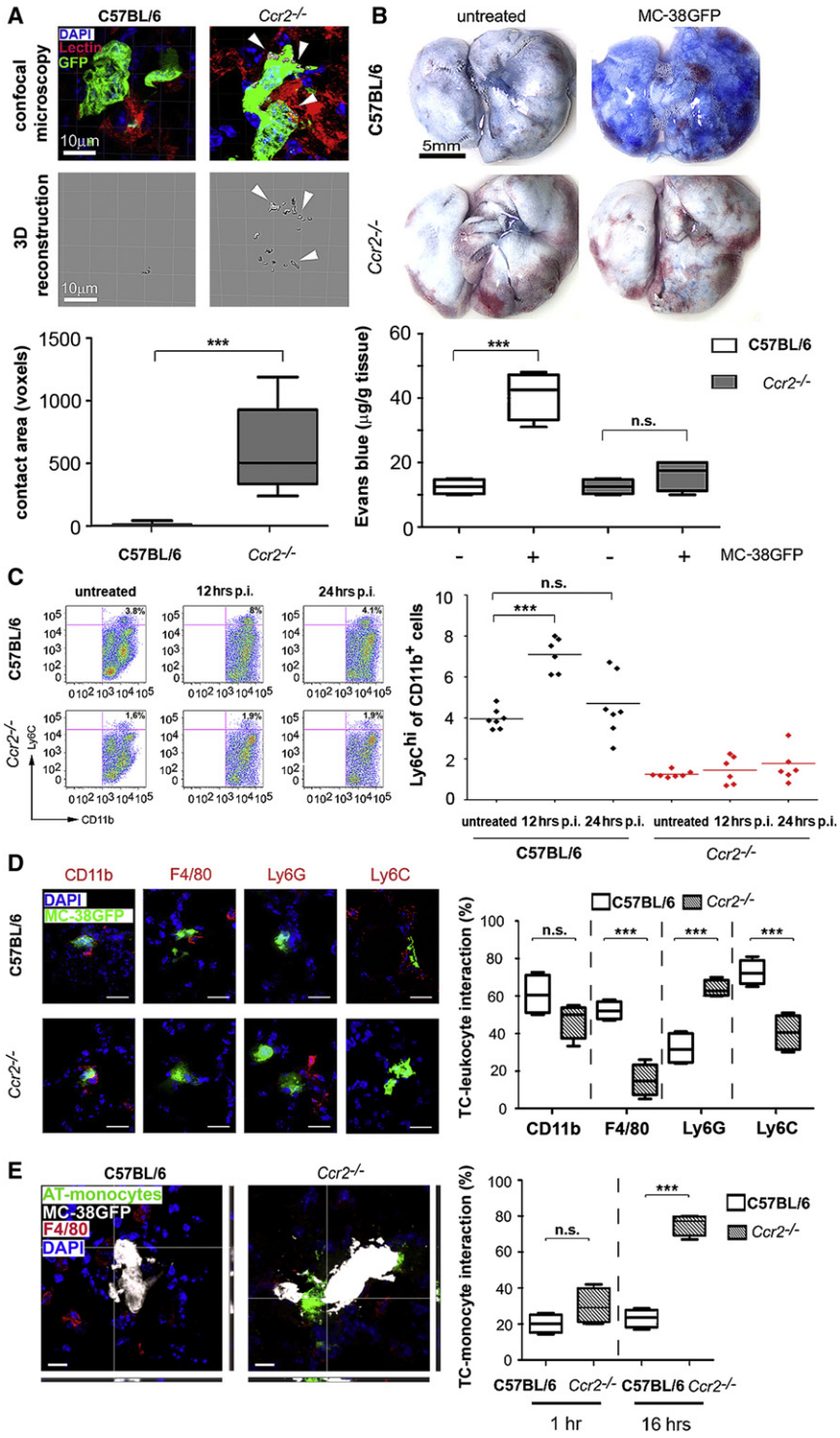

Figure 2. CCR2 Deficiency Reduces Tumor Cell Extravasation and Vascular Permeability and Affects Myeloid-Tumor Cell Interaction

(A) Confocal microscopy of MC-38GFP cells (green) and endothelial cells (red; lectin$^+$) in C57BL/6 and *Ccr2*$^{-/-}$ lungs (n = 5) 24 hr p.i. with MC-38GFP cells (upper row). Size of scale bar is indicated. Three-dimensional reconstruction of the interaction of both cell types (lower row). Quantification of the 3D contact area in voxels is shown as percentiles.

(B) Macroscopy of naive C57BL/6 and *Ccr2*$^{-/-}$ lungs (upper row) as well as 24 hr p.i. with MC-38GFP cells (lower row) upon Evans blue administration. Size of scale bar is indicated. Spectrophotometric quantification of Evans blue extracted from C57BL/6 and *Ccr2*$^{-/-}$ lungs (n = 6, each).

(C) Flow cytometry analysis for CD11b$^+$Ly6C^{hi} cells in lung tissue upon tumor cell challenge of C57BL/6 and *Ccr2*$^{-/-}$ mice over time (left panel). Quantification of Ly6C^{hi} cells is presented in the right panel (n = 6–7).

(D) Confocal microscopy images of the interaction of myeloid cells (CD11b, F4/80, Ly6G, Ly6C; all stained in red) with MC-38GFP cells (green) in C57BL/6 and *Ccr2*$^{-/-}$ mice 24 hr p.i. are shown. Nuclei are stained in blue (DAPI; left panel). Quantification of the myeloid-tumor cell interaction in lungs; percentiles are indicated (n = 3, each). Scale bar: 20 μm (right panel).

(E) Confocal microscopy analysis of the interaction of adoptively transferred, PKH26-labeled monocytes (green) with MC-38GFP cells (white) and endogenous F4/80$^+$ macrophages (red) in C57BL/6 and *Ccr2*$^{-/-}$ mice (n = 3) 16 hr p.i. (left panel). Scale bar: 10 μm; Z-stacks are indicated. Quantification of myeloid-tumor cell interaction in lungs; percentiles are indicated (right panel; mean with min/max). Statistics: ***p < 0.001; n.s., not significant.

See also Figure S2.

MC-38GFP cells in the lung vasculature were found in either genotype as early as 30 min p.i. (Figure 1G). At later time points (24, 72 hr), numbers of MC-38GFP cells in lung tissue decreased in both genotypes, though slightly more pronounced in *Ccr2*$^{-/-}$ mice at 24 hr. Besides, no significant changes were found in the structure and organization of the CD31$^+$ alveolar vasculature in both genotypes (Figure S1H).

CCR2 Controls Endothelial Permeability and Tumor Cell Extravasation

Reduced lung metastasis in *Ccr2*$^{-/-}$ mice could be explained by an impaired ability of MC-38GFP cells to extravasate into parenchyma of *Ccr2*$^{-/-}$ lungs. Confocal microscopy revealed that MC-38GFP cells remained associated with tomato lectin-stained endothelium of blood vessels in *Ccr2*$^{-/-}$ lungs at 24 hr p.i. (Figure 2A). In contrast, there was minimal contact of MC-38GFP cells with endothelia in C57BL/6 mice at 24 hr p.i., indicating that tumor cells had already extravasated from blood vessels. Three-dimensional reconstruction of confocal images showed increased contact of MC-38GFP cells with endothelium in *Ccr2*$^{-/-}$ lungs compared to C57BL/6 (p < 0.001; Figure 2A). To determine whether reduced capacity of MC-38GFP cells to extravasate in *Ccr2*$^{-/-}$ lungs was due to decreased vascular permeability, we

tested the ability of Evans blue to permeate lung tissue. No Evans blue leakage occurred in naive lungs of either genotype, indicating full vascular integrity (Figure 2B). However, 24 hr p.i. with MC-38GFP cells C57BL/6 lungs readily took up Evans blue, whereas *Ccr2*$^{-/-}$ lungs remained white, indicating no increase in vascular permeability (Figure 2B). Quantification of Evans blue confirmed the macroscopic data ($p < 0.001$; Figures 2B and S2C). The increase in vascular permeability upon injection of MC-38GFP cells was transient, as revealed by time course analyses (Figures S2A and S2B).

Next, the hypothesis whether reduced capacity of MC-38GFP cells to extravasate in *Ccr2*$^{-/-}$ lungs correlates with reduced recruitment of leukocytes was tested (Läubli et al., 2006; Qian et al., 2011). Flow cytometry of lungs from mice injected with MC-38GFP cells revealed recruitment of Ly6C^{hi} cells in C57BL/6 mice that was strongly reduced in *Ccr2*$^{-/-}$ mice (Figure 2C). The increase of Ly6C^{hi} cells in C57BL/6 lungs persisted for approximately 12–24 hr p.i. No significant increase of other immune cell types (e.g., CD4^{+}, CD8^{+}, CD11c^{+}, NK1.1^{+}) was found (data not shown).

In addition, we investigated whether lung-infiltrating myeloid cell populations are recruited to MC-38GFP cells at sites of vascular arrest. F4/80^{+}, CD11b^{+}, and Ly6C^{+} cells associated less with tumor cells in *Ccr2*$^{-/-}$ lungs compared to C57BL/6. In contrast, increased association of Ly6G^{+} cells with MC-38GFP cells was observed in *Ccr2*$^{-/-}$ lungs ($p < 0.001$; Figure 2D).

Finally, to test whether MC-38GFP cells injected into *Ccr2*$^{-/-}$ mice would still efficiently recruit myeloid cells, we adoptively transferred myeloid cells to mice 6 hr post-tumor cell injection. MC-38GFP cells recruited transferred myeloid cells in *Ccr2*$^{-/-}$ but not in C57BL/6 lungs ($p < 0.001$; Figure 2E) as MC-38GFP cells in C57BL/6 lungs had already recruited endogenous myeloid cells.

CCR2 Expression on Radio-Resistant Cells Enables Efficient Metastasis

We next tested whether reconstitution of *Ccr2*$^{-/-}$ mice with CCR2^{+} BM cells could restore the ability of MC-38GFP cells to extravasate and metastasize into lungs. Reciprocal BM reconstitutions (C57BL/6 → *Ccr2*$^{-/-}$; *Ccr2*$^{-/-}$ → C57BL/6) and controls (C57BL/6 → C57BL/6; *Ccr2*$^{-/-}$ → *Ccr2*$^{-/-}$) were performed and blood was analyzed for the presence of CCR2^{+}Ly6C^{hi} monocytes 6–8 weeks after reconstitution (Figures 3A and S3A). MC-38GFP cells were administered to reconstituted mice (efficiency >90%) and analyzed for tumor growth in lungs (Figures 3A and S3B). C57BL/6 → C57BL/6 mice displayed robust metastasis similar to control C57BL/6 mice, whereas *Ccr2*$^{-/-}$ → *Ccr2*$^{-/-}$ mice lacked or had strongly reduced metastasis. CCR2 expression on radio-resistant cells (*Ccr2*$^{-/-}$ → C57BL/6) resulted in more metastasis when compared to mice devoid of CCR2 expression in the stromal compartment (C57BL/6 → *Ccr2*$^{-/-}$; $p < 0.05$). This indicates that both, hematopoietic and stromal CCR2 expression is required for efficient metastasis.

To delineate the role of stromal CCR2 expression during metastasis, we assessed whether endothelial cell-restricted CCR2 expression (i.e., Tie2CCR2/*Ccr2*$^{-/-}$ mice; (Mildner et al., 2009) would enable tumor cell extravasation and metastasis. Tie2CCR2/*Ccr2*$^{-/-}$ mice lacked Ly6C^{hi} monocytes in blood and lung tissue and lacked CCR2 expression on CD11b^{+}, CD19^{+} or CD3^{+} cells in blood, spleen and BM (Figures 3B and S3C). Transcriptional analysis indicated *Ccr2* expression in whole lung tissue and in purified lung endothelial cells in Tie2CCR2/*Ccr2*$^{-/-}$ mice (Figures S3D and S3E). Upon injection with MC-38GFP cells, tumor cell extravasation and metastasis was partially restored in Tie2CCR2/*Ccr2*$^{-/-}$ compared to C57BL/6 mice (Figure 3C). Quantification of metastatic foci, GFP fluorescence and immunohistochemistry confirmed these data (Figures 3C, 3D, and S3F). Hence, expression of CCR2 on endothelial cells was sufficient to partially restore metastasis.

CCR2 Expression on Myeloid Cells Contributes to Tumor Cell Metastasis

To assess the role of CCR2 on myeloid cells during metastasis, we bred *Ccr2*$^{loxP/loxP}$ with *LysMCre* mice (Clausen et al., 1999), resulting in mice with reduced CCR2 expression on myeloid cells. Similar amounts of Ly6C^{hi} monocytes were detected in blood from *LysMCreCcr2*$^{loxP/loxP}$ and C57BL/6 mice by flow cytometry (Figure 4A).

We next challenged *LysMCreCcr2*$^{loxP/loxP}$ mice with MC-38GFP cells and quantified Ly6C^{hi} monocytes in lungs at 6 and 12 hr p.i. (Figures 4B and S4A). Strong reduction (>90%) in the influx of Ly6C^{hi} monocytes to the lungs and a decrease in local recruitment of F4/80^{+} and CD11b^{+} cells to tumor cells were observed (Figure 4C). To determine the effect of reduced CCR2^{+}/Ly6C^{hi} monocyte recruitment on metastasis, *LysMCreCcr2*$^{loxP/loxP}$, *Ccr2*$^{loxP/loxP}$, *Ccr2*$^{-/-}$, and C57BL/6 mice were injected with MC-38GFP and analyzed 28 d.p.i. Lung metastasis was increased in *LysMCreCcr2*$^{loxP/loxP}$ compared to *Ccr2*$^{-/-}$ mice ($p < 0.05$; Figures 4D and S4B). However, in comparison to C57BL/6 mice, metastasis in *LysMCreCcr2*$^{loxP/loxP}$ mice was decreased. This was confirmed by quantification of GFP fluorescence and immunohistochemistry of lung tissues (Figures 4D and S4C). Thus, CCR2 expression on myeloid cells contributes to metastasis of MC-38GFP cells.

Tumor Cell-Derived CCL2 Expression Controls Myeloid Cell Recruitment

Whether CCR2-dependent lung metastasis occurs also with different tumor cells, we injected mice with Lewis lung carcinoma cells (3LL). Similar to MC-38GFP cells, attenuation of metastasis was observed in *Ccr2*$^{-/-}$ when compared to C57BL/6 lungs ($p < 0.05$; Figure 5A, upper panels). Next, we injected B16-BL6 melanoma cells. Of note, similar extent of lung metastasis was observed in C57BL/6 and *Ccr2*$^{-/-}$ mice indicating that B16-BL6 melanoma cells extravasate and metastasize independently of CCR2 (Figure 5A, lower panels).

The dependency of metastasis on host-derived CCR2 expression indicates the involvement of tumor cell-intrinsic factors. We therefore first compared chemokine and chemokine receptor *mRNA* expression levels in lungs of C57BL/6 and *Ccr2*$^{-/-}$ mice injected with MC-38GFP cells. A strong increase in *Ccl2*, *Ccl7*, *Ccl12*, *Cxcl1*, and *Cxcl10* expression was detected at 4 hr p.i. in C57BL/6 lungs (Figure 5B). These transcripts remained abundant 8 and 12 hr p.i. and decreased at 48 hr p.i. (Figure 5B and data not shown). Similar transcriptional changes occurred in lungs of MC-38GFP-injected *Ccr2*$^{-/-}$mice (Figure 5B), suggesting that chemokine induction does not depend on host-derived

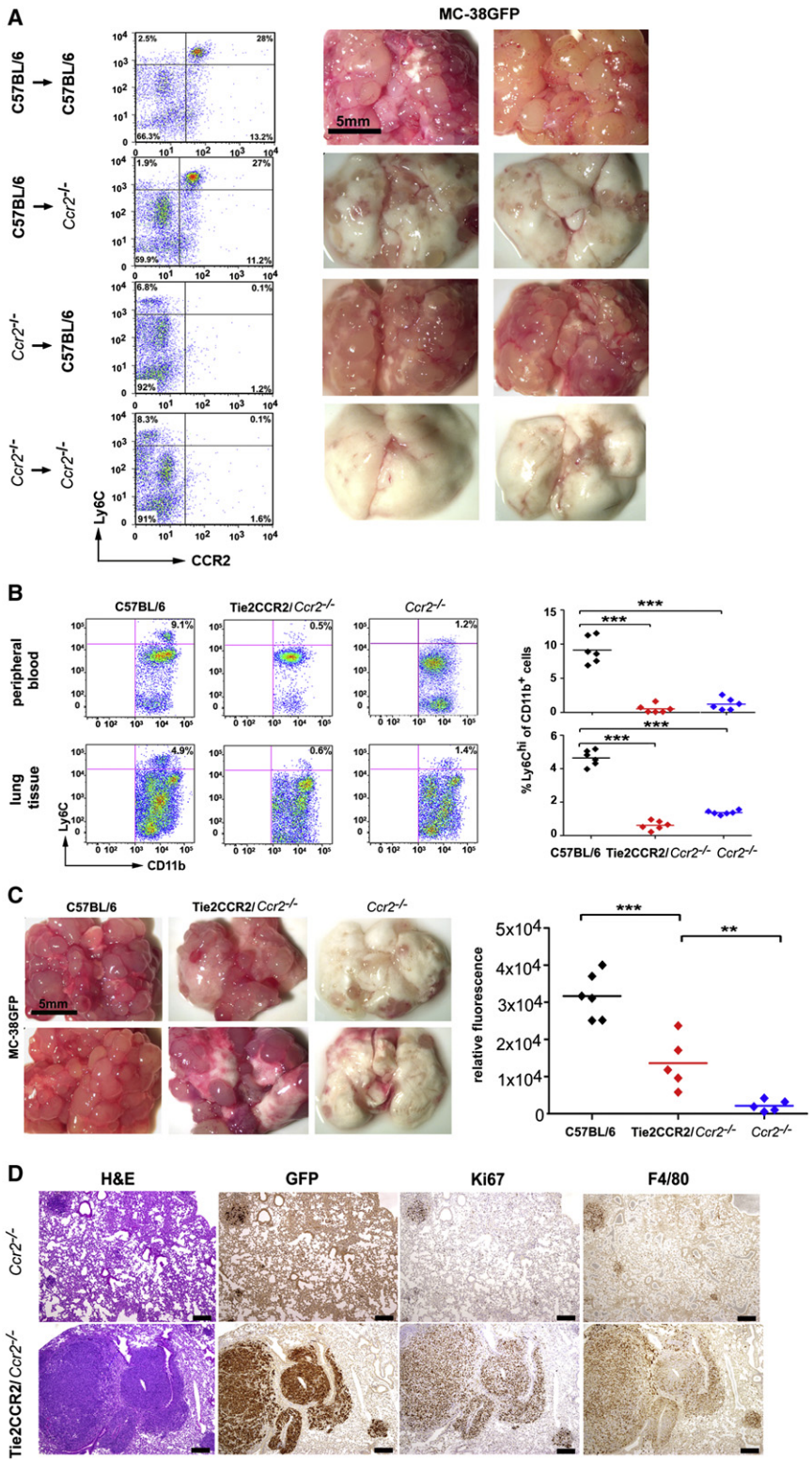

Figure 3. CCR2 Expression on Radio-Resistant Cells Suffices for Tumor Cell Metastasis

(A) Flow cytometry analysis of blood from C57BL/6→C57BL/6 (n = 8), C57BL/6→*Ccr2*$^{-/-}$ (n = 9), *Ccr2*$^{-/-}$→C57BL/6 (n = 7) and *Ccr2*$^{-/-}$→*Ccr2*$^{-/-}$ (n = 5) chimeric mice for the presence of CCR2^{+} Ly6C^{hi} cells (left row). Macroscopy of lungs from MC-38GFP-injected chimeric mice 28 d.p.i. Size of scale bar is indicated (middle/ right row).

(B) Flow cytometry for CD11b^{+}Ly6C^{hi} cells in blood (upper row) and lungs (lower row) of naive C57BL/6, Tie2CCR2/*Ccr2*$^{-/-}$ and *Ccr2*$^{-/-}$ mice (left panel). Quantification of Ly6C^{hi} cells is presented in the right panel (n = 6, each).

(C) Macroscopy of lungs from MC-38GFP-injected C57BL/6, Tie2CCR2/*Ccr2*$^{-/-}$ and *Ccr2*$^{-/-}$ mice 28 d.p.i. Size of scale bar is indicated (left panel). Quantification of GFP fluorescence in lung homogenates of C57BL/6, Tie2CCR2/*Ccr2*$^{-/-}$ and *Ccr2*$^{-/-}$ mice (n = 5, each; right panel).

(D) Histological analysis of MC-38GFP tumors in lungs of Tie2CCR2/*Ccr2*$^{-/-}$ and *Ccr2*$^{-/-}$ mice. H&E: Hematoxylin/Eosin, GFP: tumor cells, Ki67: proliferating cells, F4/80: macrophages. Scale bar: 50 μm; statistics: ***p < 0.001; **p < 0.01.

See also Figure S3.

CCR2. Alternatively, tumor cells may directly cause increased chemokine expression by altering the cellular composition and/or activation status of cells in the lungs of MC-38GFP-injected mice. However, chemokine receptor *mRNA* expression was unaltered in lungs of C57BL/6 and *Ccr2*$^{-/-}$ mice p.i. (Figure 5C). When we compared chemokine expression in MC-38GFP, 3LL, and B16-BL6 cells, elevated levels of *Ccl2*, *Ccl7*, *Cxcl1*, and *Cxcl10* transcripts were detected in MC-38GFP tumor cells compared to C57BL/6 colon (Figure S5A). Of note, *Ccl2 mRNA* and protein levels were elevated in MC-38GFP and 3LL cells and low in B16-BL6 melanoma cells, indicating that CCR2-dependent metastasis relies on tumor cell-derived CCL2 (Figures 5D, S5B, and S5C).

To determine whether MC-38 and 3LL-derived CCL2 was required for tumor cell extravasation and metastasis, CCL2 expression was silenced with small hairpin RNA (shRNA) in MC-38GFP cells (MC-38GFP^{CCL2kd}). *Ccl2 mRNA* was reduced by 75%–90%, CCL2 protein was reduced by 60%–85%, and expression of other chemokines/cytokines remained unaffected (Figure 5D). Cells stably transduced with scrambled shRNA served as control (MC-38GFP^{scr}). MC-38GFP and MC-38GFP^{CCL2kd} cells were injected into C57BL/6 mice, and their ability to recruit Ly6C^{hi} monocytes to the lung at 4 and 12 hr p.i. was assayed by flow cytometry. Similar numbers of Ly6C^{hi} cells were detected at 4 hr p.i. in lungs of C57BL/6 mice injected with MC-38GFP^{CCL2kd} or MC-38GFP cells (Figure 5E). However, no specific recruitment of Ly6C^{hi} monocytes

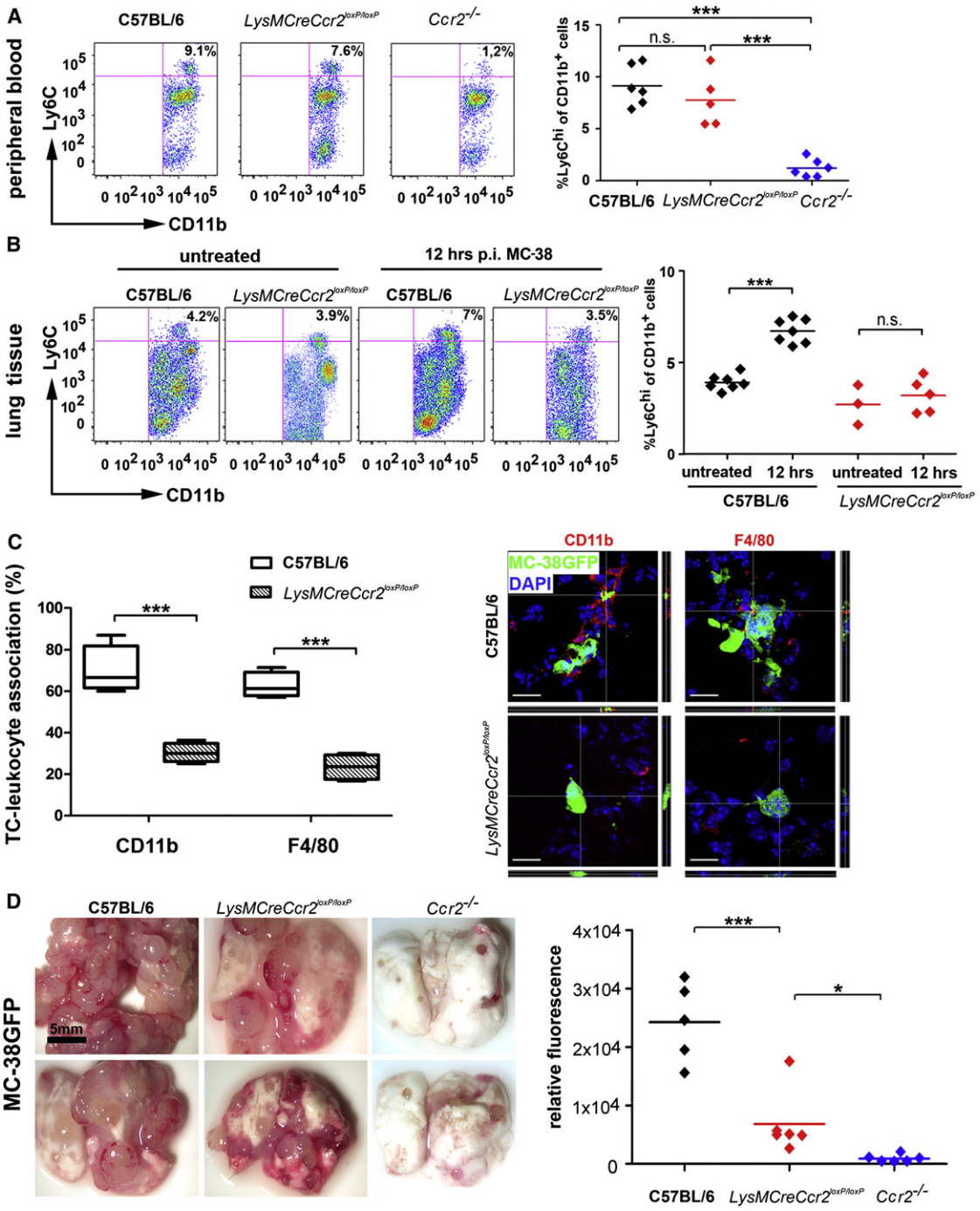

Figure 4. CCR2 Expression on Ly6C^{hi} Monocytes Facilitates Tumor Cell Extravasation

(A) Flow cytometry for CD11b^{+}Ly6C^{hi} cells in blood of C57BL/6, *LysMCreCcr2*$^{loxP/loxP}$ and *Ccr2*$^{-/-}$ mice (n = 5–6; left panel). Quantification of Ly6C^{hi} cells (right panel).

(B) Flow cytometry for CD11b^{+}Ly6C^{hi} cells in lungs of naive C57BL/6 and MC-38-injected C57BL/6 and *LysMCreCcr2*$^{loxP/loxP}$ mice 12 hr p.i. (n = 5–7; left panel). Quantification of Ly6C^{hi} cells (right panel).

(C) Confocal microscopy investigating the interaction of myeloid cells (CD11b, F4/80; red) and tumor cells (green) in lungs of C57BL/6 and *LysMCreCcr2*$^{loxP/loxP}$ mice. Nuclei are stained in blue (DAPI); scale bar: 20 μm; Z-stacks are indicated.

(D) Macroscopy of lungs from C57BL/6, *LysMCreCcr2*$^{loxP/loxP}$ and *Ccr2*$^{-/-}$ mice 28 d.p.i. with MC-38GFP. Size of scale bar is indicated (left panel). Quantification of GFP fluorescence in lung homogenates of C57BL/6 (n = 5), *LysMCreCCR2*$^{loxP/loxP}$ (n = 6), and *Ccr2*$^{-/-}$ (n = 6) mice (right panel). Statistics: ***p < 0.001; *p < 0.05; n.s., not significant.

See also Figure S4.

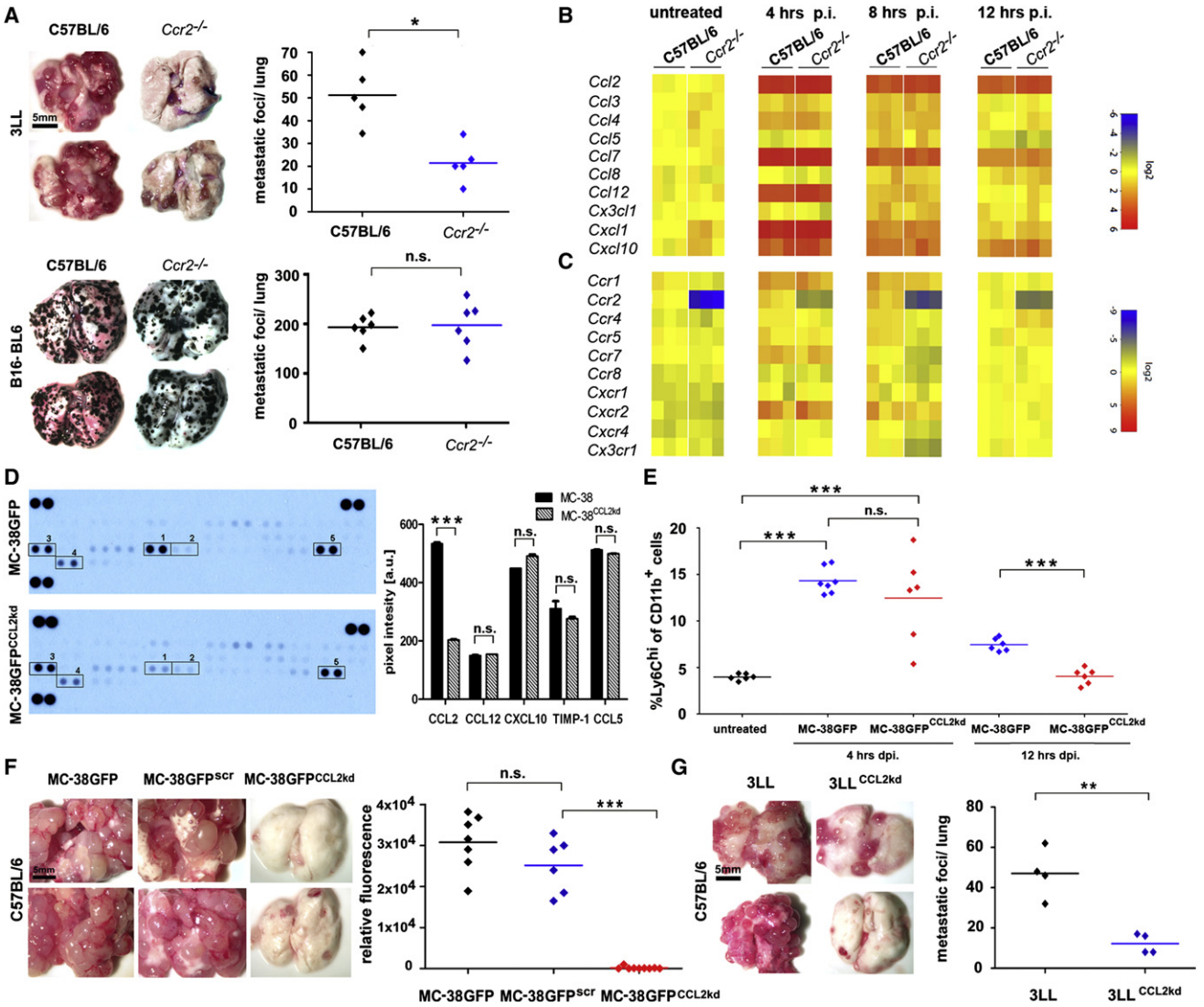

Figure 5. Tumor Cell-Derived CCL2-Dependent and -Independent Mechanisms of Tumor Cell Extravasation

(A) Macroscopy of lungs from C57BL/6 and *Ccr2*$^{-/-}$ mice at 12 d.p.i. with Lewis lung carcinoma cells (3LL) and quantification of tumor nodules (n = 5, each; upper row). Macroscopy of lungs from C57BL/6 and *Ccr2*$^{-/-}$ mice at 14 d.p.i. with melanoma cells (B16-BL6) and quantification of tumor numbers (n = 6, each; lower row).

(B and C) Real-time PCR analysis for the expression of selected chemokines (B) and chemokine receptors (C) in lungs of C57BL/6 and *Ccr2*$^{-/-}$ mice. Untreated, 4 hr p.i., 8 hr p.i., and 12 hr p.i. with MC-38GFP are shown from left to right. Data are presented as ΔΔct values in a log2 scale (red: upregulated; blue: down-regulated). Columns indicate individual mice (n = 3); rows represent particular genes. Each data point reflects the median expression of a particular gene resulting from three to four technical replicates, normalized to the mean expression value of the respective gene in C57BL/6 lungs.

(D) Expression profile of various chemokines and cytokines in MC-38GFP and MC-38GFP^{CCL2kd} cells. 1: CCL2 (silenced); 2: CCL12; 3: CXCL10; 4: TIMP-1; 5: CCL5 remain unaffected. Dots in the upper right and left corners serve as loading controls (left panel). Quantification of pixel density (shown in arbitrary units [a.u.]; mean ± SEM; right panel).

(E) Quantification of CD11b^{+}Ly6C^{hi} cells in lungs of naive C57BL/6 mice and 4 hr and 12 hr p.i. with MC-38GFP and MC-38GFP^{CCL2kd} cells (n = 6–7).

(F) Macroscopy of lungs derived from C57BL/6 mice 28 d.p.i. with MC-38GFP, MC-38GFP^{scr} and MC-38GFP^{CCL2kd} cells. Size of scale bar is indicated. Quantification of GFP fluorescence in lung homogenates of C57BL/6 mice 28 d.p.i. with MC-38GFP (n = 7), MC-38GFP^{scr} (n = 6) and MC-38GFP^{CCL2kd} (n = 9) cells.

(G) Macroscopy of lungs from C57BL/6 mice 12 d.p.i. with 3LL and 3LL^{CCL2kd} cells. Size of scale bar is indicated (left panel). Quantification of tumor nodules (n = 4, each; right panel); statistics: ***p < 0.001; **p < 0.01; *p < 0.05; n.s., not significant.

See also Figure S5.

was detected in lungs of C57BL/6 mice 12 hr p.i. with MC-38GFP^{CCL2kd} cells. Therefore, specific recruitment of Ly6C^{hi} cells is controlled by MC-38-derived CCL2. Next, we analyzed tumor cell extravasation and metastasis in C57BL/6 mice injected with MC-38GFP^{CCL2kd}, MC-38GFP or MC-38GFP^{scr} cells. Reduced lung metastasis was observed in C57BL/6 mice upon

MC-38GFP^{CCL2kd} injection and confirmed by analysis of GFP fluorescence ($p < 0.001$; Figure 5F). Similar results were obtained by silencing of CCL2 in 3LL cells ($p < 0.01$; Figure 5G).

In addition, reduced CCL2 expression in MC-38GFP cells (MC-38GFP^{CCL2kd}) diminished the ability to interact with CD11b$^+$, F4/80$^+$, or Ly6C$^+$ cells ($p < 0.001$). Although MC-38GFP^{CCL2kd} cells showed enhanced interaction with Ly6G$^+$ cells ($p < 0.001$; Figure S5D), they failed to recruit adoptively transferred myeloid cells (Figure S5E). This supports the conclusion that tumor cell-derived CCL2 is required for the association of tumor cells with myeloid cells.

CCR2 Expression on Endothelial Cells Determines Lung Permeability

To determine whether endothelial CCR2 expression was sufficient to induce vascular permeability, we injected Tie2CCR2/*Ccr2*$^{-/-}$ mice with MC-38GFP cells. Elevated levels of Evans blue in Tie2CCR2/*Ccr2*$^{-/-}$ lungs suggest that endothelial CCR2 activation is sufficient to induce lung vascular permeability (Figure 6A). Since host-derived CCL2 has been implicated in metastasis (Qian et al., 2011), we injected *Ccl2*$^{-/-}$ mice with MC-38GFP cells. Interestingly, lung vascular permeability was increased upon tumor cell injection ($p < 0.001$; Figure 6A), indicating that tumor cells induce vascular permeability in the absence of host-derived CCL2. In line, MC-38GFP^{CCL2kd} cells failed to induce vascular permeability in C57BL/6 lungs (Figure 6A). To investigate whether the local microenvironment (e.g., CCL2 expression; monocytes; stromal cells) rescues the inability of CCL2-deficient tumor cells to extravasate and metastasize, we coinjected MC-38 and MC-38GFP^{CCL2kd} cells into C57BL/6 mice. Similar numbers of metastases were observed in lungs of C57BL/6 mice injected with MC-38 versus MC-38GFP^{CCL2kd}/MC-38 cells 28 d.p.i. ($p = 0.6$; Figure 6B). Of note, lungs from C57BL/6 mice injected with MC-38GFP^{CCL2kd}/MC-38 cells displayed mainly GFP-negative tumors, suggesting that tumors mainly originated from CCL2$^+$ tumor cells ($p < 0.001$; Figures 6B and 6C). Therefore, the inability of MC-38GFP^{CCL2kd} cells to metastasize cannot be restored by the local environment.

We next examined lungs from C57BL/6 and *Ccr2*$^{-/-}$ mice 12 hr p.i. with MC-38 cells at ultrastructural level. Injection of MC-38 cells induced changes in C57BL/6 lung tissue including increased thickness of airway epithelial cells in the bronchi and thickened smooth muscle cells. Of note, tumor cells were found inside the alveoli (Figure 6D, left panel) and rarely in the vessels. Alveoli in C57BL/6 lungs appeared shrunken, with numerous alveolar macrophages and type I, II pneumocytes. Moreover, we observed an intimate interaction between MC-38 cells and C57BL/6 endothelia with tumor cell protrusions spanning through the apical side of the endothelium resembling ongoing tumor cell transmigration (Figure 6D, middle panel, inset). In contrast, *Ccr2*$^{-/-}$ lung endothelium appeared to be less affected by the injection of MC-38 tumor cells with no visible indication for endothelial attachment (Figure 6D, right panel, inset).

Endothelial CCR2 Signaling Controls Tumor Cell Extravasation through the JAK2-Stat5 and p38MAPK Pathways

To identify the mechanisms involved in tumor cell extravasation, we next examined transmigration of tumor cells through lung endothelial monolayers in presence or absence of monocytes in vitro. MC-38GFP cells incubated on C57BL/6 endothelial cells for 16 hr transmigrated only minimally toward an FCS gradient. Cocultivation of MC-38GFP cells with BM-derived monocytes induced efficient transmigration of MC-38GFP cells through C57BL/6 endothelia ($p < 0.001$; Figure 7A). In contrast, MC-38GFP cells were unable to transmigrate through endothelial cells isolated from *Ccr2*$^{-/-}$ mice either in the presence or absence of monocytes ($p = 0.6$; Figure 7A). To determine whether tumor cell transmigration depends on tumor cell-derived CCL2, we tested the ability of MC-38GFP^{CCL2kd} cells to transmigrate in vitro. MC-38GFP^{CCL2kd} cells could not transmigrate through a C57BL/6 endothelial monolayer in the presence of monocytes ($p < 0.001$; Figure 7B). Interestingly, neither lack of endothelial nor monocytic CCR2 expression affected efficacy of monocyte transmigration (Figure 7C). Taken together, endothelial CCR2 signaling can specifically enable transmigration of tumor cells without affecting monocytes. Tumor cell-derived CCL2 was sufficient to induce permeability in the CCR2$^+$ endothelial monolayer even in the absence of monocytes. In contrast, MC-38GFP^{CCL2kd} cells induced partial endothelial permeability only in the presence of monocytes (Figure 7D). These findings provide direct evidence for the role of endothelial CCR2 activation during tumor cell extravasation; and for the supportive role of monocytes in this process.

CCL2 is known to activate Janus kinase 2 (JAK2) through CCR2 (Mellado et al., 1998), thereby triggering several downstream pathways such as Stat1, Stat3 and Stat5, p38MAPK, and PI3K (Agrawal et al., 2011; Sanz-Moreno et al., 2011). We first tested whether inhibition of JAK2 phosphorylation would affect tumor cell transmigration. AG490 effectively blocked tumor cell transmigration, demonstrating the requirement of CCR2-JAK2 signaling for tumor cell extravasation ($p < 0.001$; Figure 7E). Inhibition of Stat3 phosphorylation (S3I-201) failed to affect tumor cell migration ($p = 0.8$), while block of Stat5 phosphorylation impeded transmigration of MC-38GFP cells ($p < 0.001$; Figure 7E). PI3K inhibition with Wortmannin did not alter tumor cell transmigration ($p = 0.6$), whereas blocking p38MAPK phosphorylation with SB202190 did ($p < 0.001$, Figure 7F). Therefore, both JAK2-Stat5 and p38MAPK pathways appeared to be involved in transmigration of MC-38GFP cells through CCR2$^+$ endothelium.

We next addressed whether tumor cells, rather than transmigrating through endothelial junctions, might trans-invade endothelial cells (Feng et al., 1998), which was shown to depend on Rac/Rho GTPases. However, inhibition of Rac1 (with NSC23766) failed to block tumor cell transmigration pointing at transmigration through endothelial junctions (Figure 7E).

To provide further evidence that CCR2-JAK2 signaling is involved in tumor cell extravasation, we measured JAK2 phosphorylation in lung homogenates from MC-38-injected mice. Increased JAK2 phosphorylation relative to total JAK2 was observed at 8 and 12 hr p.i. in C57BL/6 lungs which was prevented by AG490. In contrast, inhibition of p38MAPK did not affect JAK2 phosphorylation (Figure 7F). Importantly, no or minor phosphorylation of JAK2 was detected in *Ccr2*$^{-/-}$ mice upon tumor cell injection, confirming that CCR2 expression in lungs is crucial for activation of this signaling cascade. Similarly, p38MAPK and Stat5 were activated in lungs of C57BL/6 mice

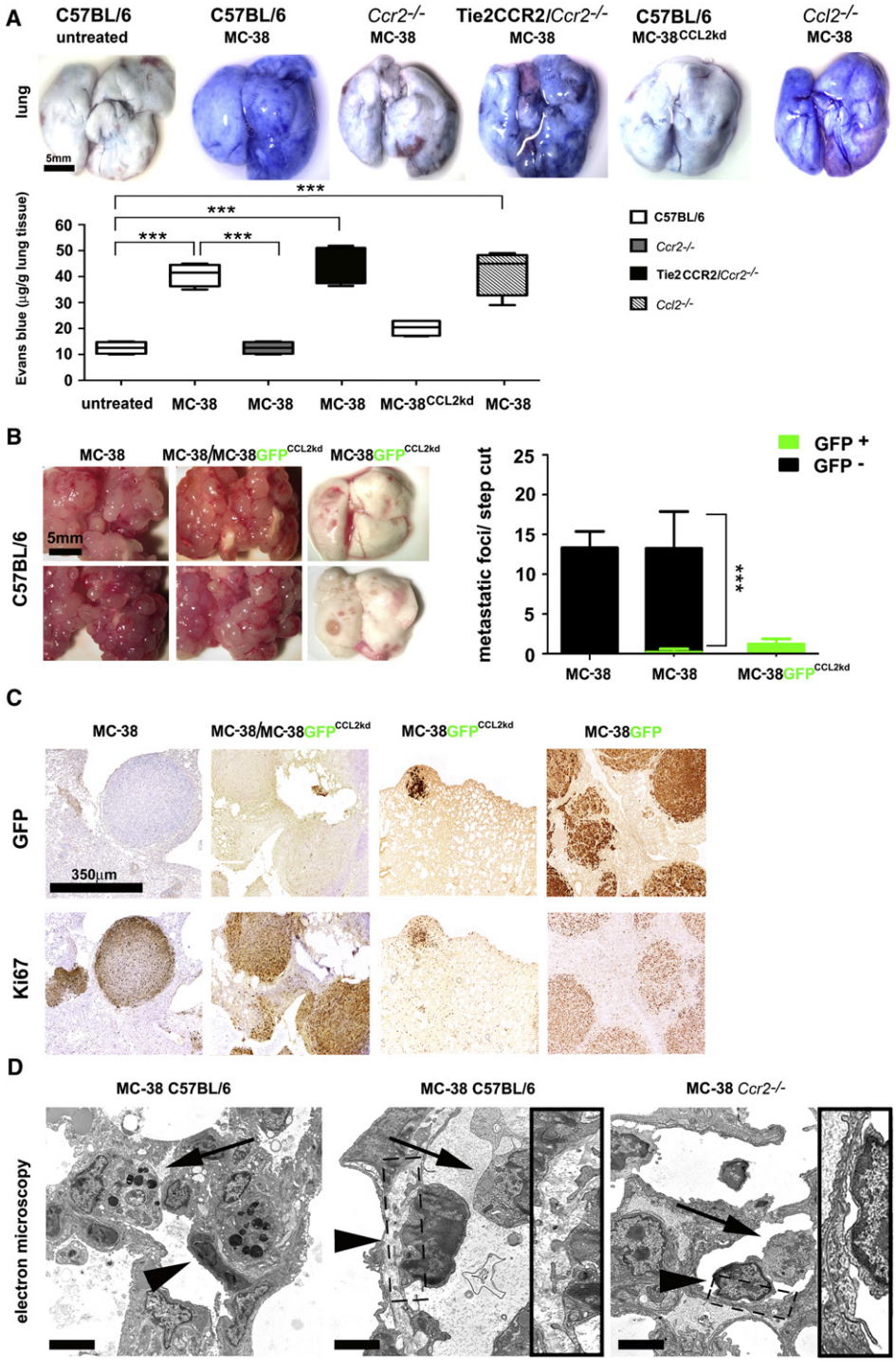

Figure 6. Tumor Cell-Derived CCL2 Is Sufficient to Induce Endothelial Permeability

(A) Macroscopy of lungs with Evans blue accumulation derived from untreated C57BL/6 mice or treated mice of various genotypes 24 hr p.i. with MC-38GFP and MC-38GFP^{CCL2kd} cells. Scale bar is indicated. Spectrophotometric quantification of Evans blue extracted from lung tissue.

(B) Macroscopy of lungs derived from C57BL/6 mice 28 d.p.i. with MC-38 (n = 3), MC-38/MC-38GFP^{CCL2kd} (1:1 ratio; n = 5) and MC-38GFP^{CCL2kd} cells (n = 3; left panel). Quantification of tumor nodules on step cuts through lungs (black bars represent MC-38 cells, green bars MC-38GFP^{CCL2kd} cells; mean ± SEM; right panel).

(C) Immunohistochemistry for the quantification of tumor nodules. GFP and Ki67 served as tumor markers. Size of scale bar is indicated.

(D) Electron microscopy images of lungs of C57BL/6 (left and middle) and *Ccr2*$^{-/-}$ mice (right) 12 hr p.i. with MC-38GFP. Left: arrowhead points toward a tumor cell in the alveolar space, in close contact to a type II pneumocyte (arrow). Middle panel: arrowhead shows an attached and transmigrating tumor cell localized within the vessel. The arrow indicates a monocyte within the vessel. The insert shows the interaction between tumor cell and vessel wall at higher magnification. Right: No visible transmigration of tumor cells (arrow head) in lungs of *Ccr2*$^{-/-}$ mice. Arrow: monocyte within the vessel. Scale bar: 5 µm; statistics: ***$p < 0.001$.

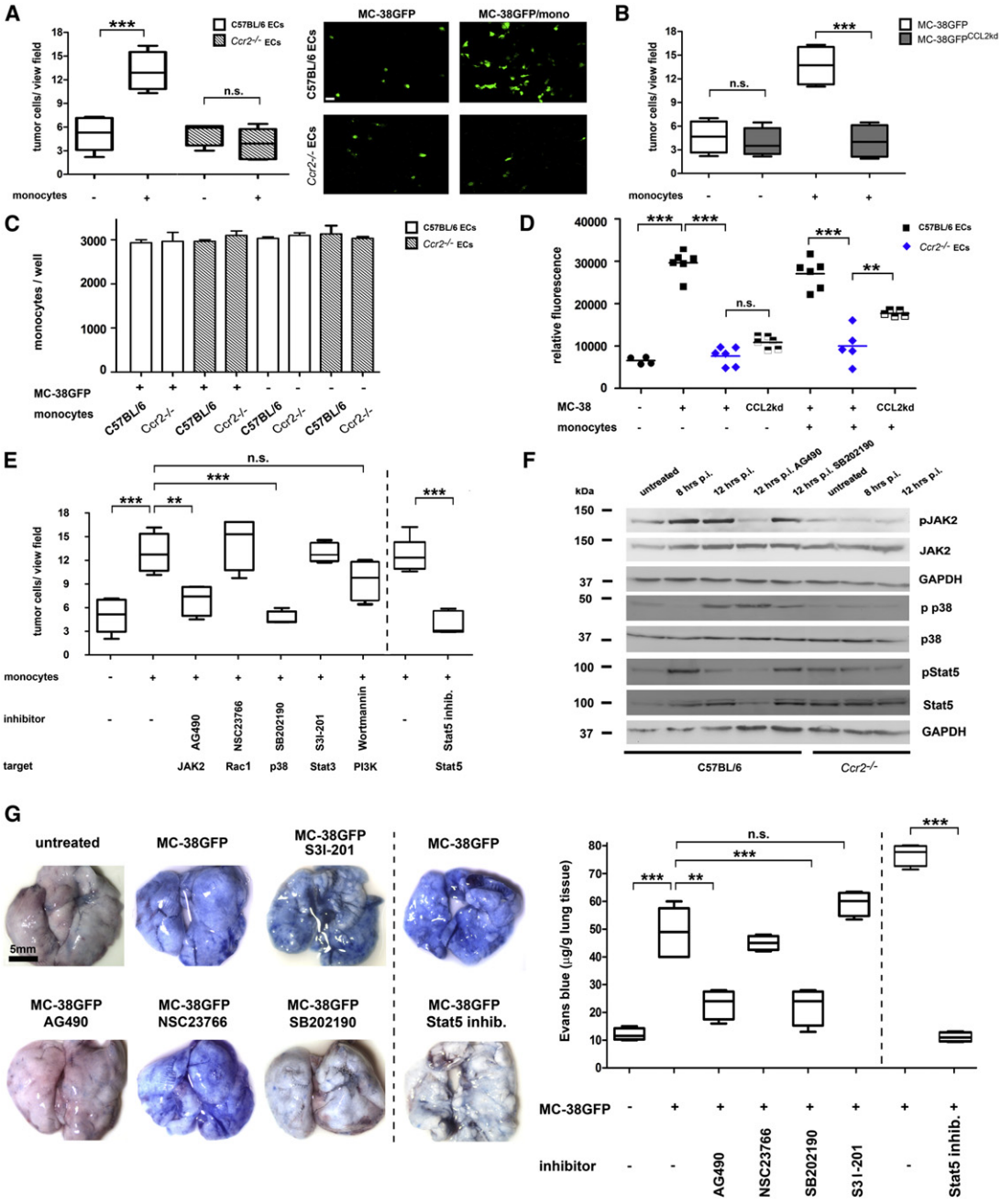

Figure 7. CCL2-CCR2-Mediated Permeabilization of the Endothelium Is Driven by JAK2-Stat5 and p38MAPK activation

(A) MC-38GFP cells were cocultured with monocytes for 16 hr on monolayers of endothelial cells derived either from C57BL/6 or *Ccr2*$^{-/-}$ lungs. Transmigrated GFP^{+} tumor cells in the lower chamber were counted and are presented as percentiles (left panel). Representative images of transmigrated tumor cells for each coculture; scale bar: 10 μm (right panel).

(B) MC-38GFP cells were compared with MC-38GFP^{CCL2kd} cells for their efficiency to migrate through C57BL/6 endothelial cells. Transmigrated GFP^{+} tumor cells were counted and values are presented as percentiles.

(C) Analysis of transmigrated monocytes at 16 hr post coculture with C57BL/6 or *Ccr2*$^{-/-}$ endothelial cells with or without tumor cells (mean ± SEM).

(D) Permeability of the C57BL/6 or *Ccr2*$^{-/-}$ endothelial cell layer for Dextran-FITC was determined at 7 hr post addition of tumor cells with or without monocytes.

(E) Inhibitors for JAK2 (AG490), Rac (NSC23766), p38MAPK (SB201290), Stat3 (S3I-201), PI3K (Wortmannin), and Stat5 pathways were added to the coculture of MC-38GFP cells with monocytes. GFP^{+} tumor cells transmigrated through the C57BL/6 endothelial cell layer were counted in the lower chamber.

(F) Immunoblot analysis of lung samples derived from C57BL/6 and *Ccr2*$^{-/-}$ mice (untreated, 8 and 12 hr p.i.) as well as C57BL/6 mice treated with AG490 or SB202190 (12 hr p.i.). Panel from top to bottom: pJAK2, JAK2, GAPDH, P-p38, p38, pStat5, Stat5, and GAPDH.

(G) Macroscopy of lungs upon Evans blue administration in presence or absence of inhibitors for Stat3, JAK2, Rac1, p38MAPK and Stat5 16 hr p.i. with MC-38GFP cells. Quantification of Evans blue (n = 4, each; right panel; mean with min/max is shown). Statistics: ***p < 0.001; **p < 0.01; n.s., not significant.

See also Figure S6.

upon tumor cell injection (between 8 and 12 hr p.i.) but not in *Ccr2*$^{-/-}$ lungs (Figure 7F).

We next tested the involvement of the above-described signaling pathways in controlling lung permeability. In line with our in vitro data, JAK2, Stat5 and p38MAPK inhibition prevented the increase in vascular permeability induced by MC-38GFP cells in C57BL/6 mice. However, treatment with Rac1 (NSC23766) and Stat3 (S3I-201) inhibitor failed to affect vascular permeability (Figure 7G). Since a specific inhibitor of PI3K did not affect tumor cell transmigration in vitro, it is unlikely that PI3K signaling is involved in tumor cell extravasation. Accordingly, PI3K$\gamma^{-/-}$ mice developed lung metastasis similar to C57BL/6 mice 28 d.p.i. of MC-38GFP cells (data not shown). Thus, inhibition of JAK2-Stat5 and p38MAPK signaling prevents tumor cell-induced vascular permeability in vivo.

We next investigated whether JAK2-Stat5 or p38MAPK inhibition exclusively affects endothelial cells or also monocytes. We therefore analyzed levels of phosphorylated Stat5 and p38MAPK in MC-38GFP-injected Tie2CCR2/*Ccr2*$^{-/-}$ mice (Figures S6A and S6B). Increase in phosphorylation of JAK2, Stat5 and p38MAPK was comparable both in Tie2CCR2/*Ccr2*$^{-/-}$ and C57BL/6 lungs. Therefore, Stat5 and p38MAPK activation in endothelial cells occurs in the absence of Ly6C^{hi} monocytes.

We next determined whether lack of CCR2 signaling in vivo would affect the expression of Stat5 and p38MAPK target genes associated with the vascular integrity of endothelial cells. Significantly decreased expression of *E-selectin* and *Icam-1* ($p < 0.05$; $p < 0.001$) was found in *Ccr2*$^{-/-}$ lungs compared to C57BL/6 at 8 hr p.i. (Figure S6C). This suggested that the proinflammatory endothelial response associated with metastasis was reduced in *Ccr2*$^{-/-}$ mice. Aside from these transcriptional changes, we observed that coincubation of primary endothelial cells with MC-38 cells caused cytoskeletal retraction and disruption of the endothelial layer, as determined by phalloidin-fluorescein isothiocyanate (FITC) staining (Figure S6D).

We next investigated on ultrastructural level, whether the inhibition of CCR2 signaling affects tumor cell behavior in lungs of C57BL/6 mice. In contrast to lungs of naive mice, but similar to C57BL/6 tumor injected mice, thickened airway epithelial cells and smooth muscle cells were found in mice treated with JAK2 inhibitor. However, strongly reduced tumor cell extravasation could be observed in AG490 treated mice (Figure 8A).

Finally, we assessed whether JAK2 and p38MAPK inhibition would also block lung metastasis. Thus, we treated MC-38GFP-injected mice with AG490 or SB202190 during the first 3 d.p.i. Blockade of both, JAK2 and p38MAPK signaling attenuated metastasis ($p < 0.05$; Figures 8B and 8C).

CCL2 Expression Correlates with Metastatic Potential in Human Colon Cancer Tissue

We next analyzed *CCL2* expression in human primary nonmetastasized colon tumors (UICC stages I and II) and in colon tumors that metastasized into the lymph nodes (UICC stage) or into distant organs (UICC stage IV). *CCL2* transcripts were more abundant in primary colon tumors of stages I, II, and III when compared to healthy colon samples. However, *CCL2* expression was particularly high in colon tumors stage IV that developed metastases in distant organs (Figure 8D), indicating that upregulation of *CCL2* correlates with metastatic potential.

DISCUSSION

During the multistep process of metastasis, cytokines and chemokines have been reported to have pro- or antitumorigenic effects (Granot et al., 2011; Qian et al., 2011). Elevated CCL2 levels have been previously linked to malignancy and increased metastasis in a number of cancers (Soria et al., 2011; Yoshidome et al., 2009; Zhang et al., 2010; Zijlmans et al., 2006). Our analysis of primary colon tumors (UICC stages I–IV) confirmed the link between CCL2 upregulation in stage IV colon carcinoma and metastatic capacity. Recent studies have shown that monocyte recruitment by CCL2 contributes to lung metastasis of breast cancer (Lu and Kang, 2009; Qian et al., 2011). Our data provide evidence that tumor cell-derived CCL2 activates CCR2 on endothelial cells, thereby enabling efficient tumor cell extravasation.

To study the mechanisms of tumor cell extravasation, we applied chimeric, transgenic, and knockout mice, as well as in vitro assays. This allowed us to define the role of tumor cell-derived CCL2 in a spatial and temporal manner. Using these models, we determined that enhanced lung vascular permeability, tumor cell extravasation, and recruitment of Ly6C^{hi} monocytes are initiated by tumor cell-derived CCL2 at sites of vascular arrest in a CCR2-dependent manner.

It was previously demonstrated that systemic depletion of CCL2 with neutralizing antibodies could attenuate metastasis, while the origin of CCL2 was identified to be in tumor cells and stromal compartment (Qian et al., 2011). We show that vascular permeability was enhanced in both *Ccl2*$^{-/-}$ and C57BL/6 mice, suggesting that host-derived CCL2 is not required. In addition, silencing of CCL2 expression in two different tumor cell lines (MC-38GFP and 3LL) prevented induction of lung vascular permeability and subsequent metastasis, further demonstrating that tumor cell-derived CCL2 is sufficient for initiation of tumor cell extravasation. Previous observations that CCL2 overexpression in tumor cells enhanced metastasis are in line with our findings (Lu and Kang, 2009). Importantly, recent work indicated that CCR2 deficiency does not affect primary tumor growth (Sawanobori et al., 2008), arguing against the possibility that the observed reduction in metastasis is the result of tumor growth rate.

Which cellular compartment integrates tumor cell-derived CCL2 signaling through CCR2? CCL2-dependent recruitment of monocytes to metastatic sites has been shown to contribute to metastasis (Mizutani et al., 2009; Qian et al., 2011). It is also known that CCL2-expressing breast tumor cells engage CCR2^{+} cells of monocytic origin to facilitate colonization of lung and bone (Lu and Kang, 2009). Consistent with this, we show that recruitment of Ly6C^{hi} monocytes correlates with metastasis. However, depletion of CCR2 from monocytes in *LysMCreCcr2*$^{loxP/loxP}$ mice strongly affected monocyte recruitment and interaction with tumor cells and consequently reduced but did not prevent metastasis. In line, even partial reduction of CCR2 affected monocyte recruitment (Leuschner et al., 2011). Accordingly, the number of metastases in *Ccr2*$^{-/-}$ → C57BL/6 chimeric mice was considerably lower than in C57BL/6 mice. Furthermore, experiments with Tie2CCR2/*Ccr2*$^{-/-}$ mice confirmed that endothelial expression of CCR2 is sufficient for metastasis (Figure 3C). Therefore, Ly6C^{hi} monocytes appear to be necessary but not sufficient for effective metastasis.

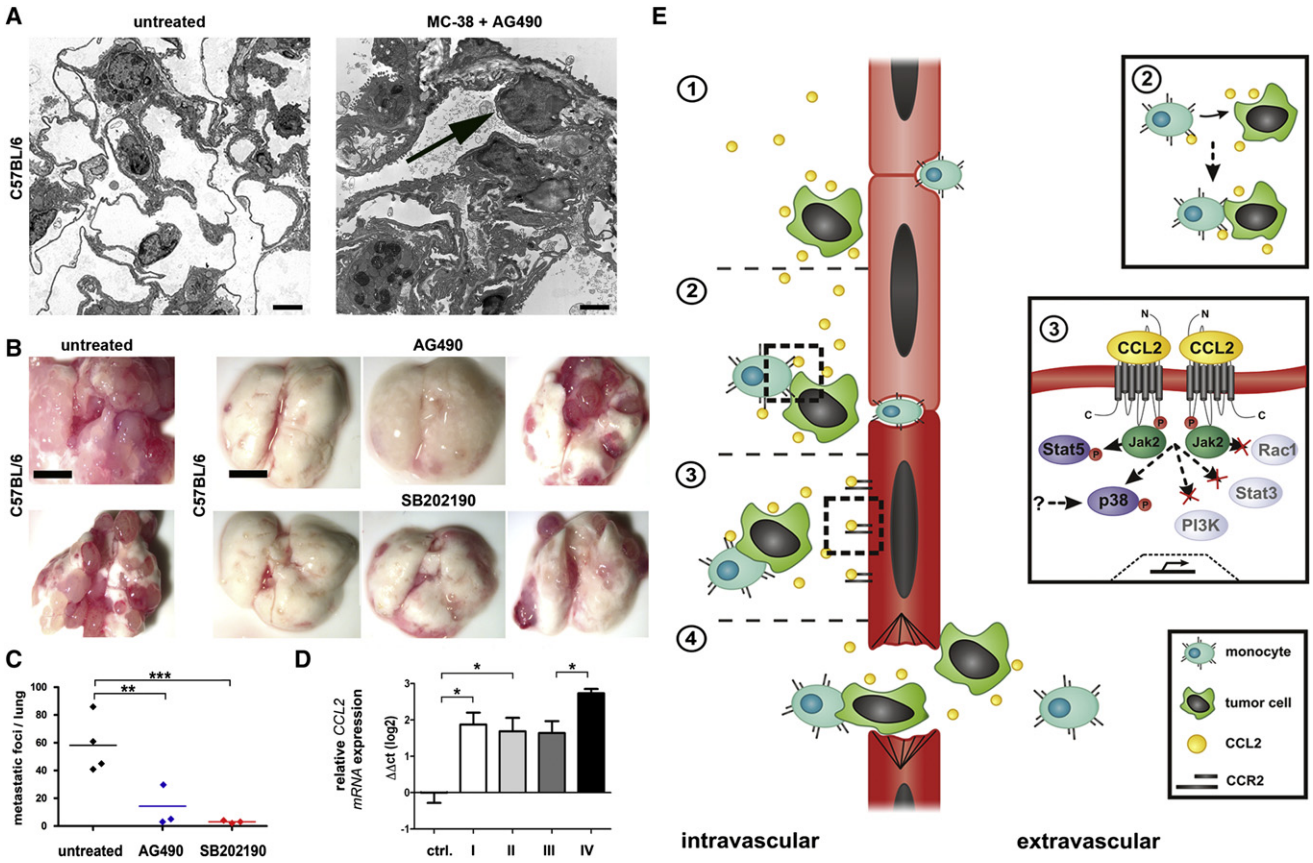

Figure 8. Short-Term Inhibition of JAK2 or p38MAPK Impedes Tumor Cell Metastasis

(A) Electron microscopy images of a naive C57BL/6 lung (left, scale bar: 4 μm) and 12 hr p.i. with MC-38GFP and AG490 treatment (right, scale bar: 2 μm); arrow points toward a tumor cell.

(B) Macroscopy of lungs from C57BL/6 mice 26 d.p.i. with MC-38GFP left untreated or with AG490 or SB202190 treatment during the first 3 d.p.i. Scale bar: 5 mm.

(C) Quantification of tumor nodules in lungs of C57BL/6 mice left untreated (n = 4), SB202190 (n = 3), or AG490 (n = 3) treated upon MC-38GFP injection.

(D) Transcriptional analysis of *CCL2* levels in tissue obtained from colon-cancer patients. *mRNA* expression levels in healthy control tissue (ctrl.; n = 4), in tumor samples classified as stage I (n = 10), stage II (n = 10) both being nonmetastatic; stage III: metastastic in lymph nodes (n = 10), stage IV: metastatic in distant organs (n = 9) colon carcinomas were studied. Data are presented in a log2 scale. Each bar reflects the median expression (mean ± SEM) of a gene resulting from three to four technical replicates, normalized to the mean expression value of *CCL2* in control samples. Statistics: ***$p < 0.001$; **$p < 0.01$; *$p < 0.05$.

(E) Schematic model depicting how CCL2-expressing tumor cells attract monocytes (1 and 2), trigger vascular permeability (3) and transmigrate through the endothelium (4). Tumor cell-dependent activation of CCR2 on the endothelium induces JAK2, Stat5, and p38MAPK phosphorylation but not PI3K, Stat3, and Rac1.

Here, we demonstrate that endothelial CCR2 signaling controls metastasis by promoting tumor cell extravasation. We hypothesize that CCR2 on endothelial cells may resemble a "lock-and-key" signal for opening the vasculature and enabling extravasation of $CCL2^+$ tumor cells. Indeed, we found that expression of CCR2 on endothelial cells is linked to the induction of vascular permeability. This "lock-and-key" relationship was dependent on CCL2 expression solely from the tumor cells, since MC-38^{CCL2kd} cells failed to induce vascular permeability and metastasis in C57BL/6 mice. Since coinjection experiments of MC-38GFP^{CCL2kd}/MC-38 cells only induced efficient metastasis of $CCL2^+$ but not MC-38GFP^{CCL2kd} cells, we suggest that an intimate interaction of $CCL2^+$ colon carcinoma cells with the $CCR2^+$ endothelium is required.

Monocyte transmigration still occurred through CCR2-deficient endothelial monolayers, indicating that CCR2 signaling on endothelial cells specifically enables transmigration of $CCL2^+$ tumor cells.

There are several signaling pathways that participate in endothelial activation associated with diapedesis of leukocytes during inflammation (McIntyre et al., 2003), some of which act downstream of CCR2 (e.g., Stat3, PI3K (Yu et al., 2009). From the panel of inhibitors tested in vitro, we identified the JAK2, Stat5, and p38MAPK signaling pathways as responsible for induction of vascular permeability and extravasation in vivo. Activation of the p38MAPK in endothelial cells by transmigrating tumor cells has been observed previously (Tremblay et al., 2006). The pattern of JAK2 and p38MAPK activation in MC-38-injected C57BL/6 mice suggests that these two pathways act independently of each other, since inhibition of p38MAPK phosphorylation did not block Stat5 or JAK2 phosphorylation. In contrast, JAK2 inhibition blocked Stat5 but not p38MAPK

phosphorylation. Tumor cell-induced phosphorylation of both JAK2-Stat5 and p38MAPK was detected in Tie2CCR2/*Ccr2*$^{-/-}$ lungs, arguing that both signaling pathways are activated in parallel in the endothelial compartment.

Based on our data, we propose the following model describing the role of CCR2 signaling in metastasis: Upon vascular arrest, CCL2^{+} tumor cells induce a local chemokine gradient, recruiting CCR2^{+} monocytes. Concomitantly or subsequently direct activation of CCR2 on the endothelium is triggered by tumor cells, which is critical for metastasis. CCL2 activates JAK2 and p38MAPK signaling, leading to enhanced vascular permeability that along with monocyte recruitment enables efficient tumor cell extravasation (Figure 8E). The exact kinetics and modes of transmigration remain to be described. Our data identify a yet undescribed role for tumor cell-derived chemokines in metastasis that goes beyond the attraction of inflammatory cells.

With increasing interest, chemokines and chemokine receptors are being considered as targets for cancer therapy, including metastasis. Certainly, the CCL2-CCR2 axis is just one possible chemokine-chemokine receptor axis exploited by tumor cells. Nevertheless, further studies will be required to identify which cancers use chemokine-chemokine receptor interactions for efficient tumor cell extravasation and metastasis. Our results identify inhibition of CCR2 and its downstream targets (JAK2/Stat5/p38MAPK) as a potential strategy for preventing CCL2-mediated metastasis therapeutically.

EXPERIMENTAL PROCEDURES

Mice

Animals were maintained under specific pathogen-free conditions, and experiments were approved by Zürich Cantonal Veterinary Committee in accordance to the guidelines of the Swiss Animal Protection Law. C57BL/6 and *Ccl2*$^{-/-}$ mice were purchased from the Jackson Laboratory, *Ccr2*$^{-/-}$ mice (Boring et al., 1997; Kuziel et al., 1997) were either purchased from the Jackson Laboratory or obtained from our own breedings; Tie2CCR2/*Ccr2*$^{-/-}$ were described previously (Mildner et al., 2009); *LysMCreCcr2*$^{loxP/loxP}$ were obtained from M. Pasparakis (G.v.L. and M.P., unpublished data); and BacCCR2GFP and BacCCR2DTCFP mice (Hohl et al., 2009) were obtained from E. Pamer.

Human Colon Cancer Tissue

Patients with colon carcinomas stage UICC I (n = 10), II (n = 10), III (n = 10), and IV (n = 9) were selected from the Erlangen Registry for Colorectal Carcinomas (ERCRC). The local ethics committee approved the study and the regulations of the same committee of the clinical center Erlangen were obeyed; written consent has been obtained (approval nr. 3914).

Experimental Metastasis Assay

Mice were i.v. injected with MC-38GFP cells (3×10^5) and euthanized after 28 days. Metastatic foci were counted, macroscopic pictures of lungs were taken and GFP fluorescence was measured in lung homogenates (Borsig et al., 2002).

Vascular Permeability Assay

Permeability of the lung microvasculature was determined with Evans blue dye extravasation technique (Reutershan et al., 2006). Briefly, mice were injected with tumor cells, and, after 24 hr, 2 mg of Evans blue was i.v. injected followed by euthanasia 30 min later. In experiments using various signaling pathways inhibitors (AG490 and SB202190 [Sigma], NSC23766 [Calbiochem], S3I-201 and Stat5 [Santa Cruz]), inhibitors were i.p. injected 1 hr before and 5 hr post tumor cell injection at concentrations of 10–25 mg/kg. Lungs were perfused with PBS, dissected, photographed and homogenized. Evans blue was extracted by incubation with formamide at 60°C for 18 hr. Evans blue concentration was measured spectrophotometrically (absorbance at 620 nm).

Statistical Analysis

Statistical analysis was performed with the GraphPad Prism software (version 4.0). All data are presented as mean ± SEM and were analyzed by ANOVA with the post hoc Bonferroni multiple comparison test, unless specified differently. Analysis of two samples was performed with Student's t test.

SUPPLEMENTAL INFORMATION

Supplemental Information includes six figures, Supplemental Experimental Procedures, and Supplemental References and can be found with this article online at http://dx.doi.org/10.1016/j.ccr.2012.05.023.

ACKNOWLEDGMENTS

We would like to thank Drs. Anna Lorentzen, Tracy O'Connor, Barbara Stecher, and Prof. Percy Knolle for critically reading the manuscript, Frank Tacke for mice, Yannick Böge, Renaud Maire, Robin Nagel, Silvia Behnke, Jay Tracy, Daniel Kull, Ruth Hillermann, Alexandra Müller, and Prof. Ursus Riede for support. M.H. was supported by an ERC Starting grant (LiverCancerMechanisms), the Helmholtz foundation, the Hofschneider foundation, Oncosuisse, and the Swiss National Foundation (no. 310030-130822). L.B. was supported by Swiss National Foundation (no. 31003A-133025). M.P. was supported by the center of chronic immunodeficiency (CCI) and the DFG (SFB 620, FOR1336, PR 577/8-1). M.S. and R.S.C. were supported by the German Federal Ministry for Education and Research.

Received: October 10, 2011
Revised: January 31, 2012
Accepted: May 18, 2012
Published: July 9, 2012

REFERENCES

Agrawal, S., Gollapudi, S., Su, H., and Gupta, S. (2011). Leptin activates human B cells to secrete TNF-α, IL-6, and IL-10 via JAK2/STAT3 and p38MAPK/ERK1/2 signaling pathway. J. Clin. Immunol. *31*, 472–478.

Allavena, P., Germano, G., Marchesi, F., and Mantovani, A. (2011). Chemokines in cancer related inflammation. Exp. Cell Res. *317*, 664–673.

Boring, L., Gosling, J., Chensue, S.W., Kunkel, S.L., Farese, R.V., Jr., Broxmeyer, H.E., and Charo, I.F. (1997). Impaired monocyte migration and reduced type 1 (Th1) cytokine responses in C-C chemokine receptor 2 knockout mice. J. Clin. Invest. *100*, 2552–2561.

Borsig, L., Wong, R., Hynes, R.O., Varki, N.M., and Varki, A. (2002). Synergistic effects of L- and P-selectin in facilitating tumor metastasis can involve non-mucin ligands and implicate leukocytes as enhancers of metastasis. Proc. Natl. Acad. Sci. USA *99*, 2193–2198.

Chambers, A.F., Groom, A.C., and MacDonald, I.C. (2002). Dissemination and growth of cancer cells in metastatic sites. Nat. Rev. Cancer *2*, 563–572.

Clausen, B.E., Burkhardt, C., Reith, W., Renkawitz, R., and Förster, I. (1999). Conditional gene targeting in macrophages and granulocytes using LysMcre mice. Transgenic Res. *8*, 265–277.

Feng, D., Nagy, J.A., Pyne, K., Dvorak, H.F., and Dvorak, A.M. (1998). Neutrophils emigrate from venules by a transendothelial cell pathway in response to FMLP. J. Exp. Med. *187*, 903–915.

Granot, Z., Henke, E., Comen, E.A., King, T.A., Norton, L., and Benezra, R. (2011). Tumor entrained neutrophils inhibit seeding in the premetastatic lung. Cancer Cell *20*, 300–314.

Gupta, G.P., and Massagué, J. (2006). Cancer metastasis: building a framework. Cell *127*, 679–695.

Hiratsuka, S., Watanabe, A., Aburatani, H., and Maru, Y. (2006). Tumour-mediated upregulation of chemoattractants and recruitment of myeloid cells predetermines lung metastasis. Nat. Cell Biol. *8*, 1369–1375.

Hohl, T.M., Rivera, A., Lipuma, L., Gallegos, A., Shi, C., Mack, M., and Pamer, E.G. (2009). Inflammatory monocytes facilitate adaptive CD4 T cell responses during respiratory fungal infection. Cell Host Microbe *6*, 470–481.

Joyce, J.A., and Pollard, J.W. (2009). Microenvironmental regulation of metastasis. Nat. Rev. Cancer *9*, 239–252.

Kim, S., Takahashi, H., Lin, W.W., Descargues, P., Grivennikov, S., Kim, Y., Luo, J.L., and Karin, M. (2009). Carcinoma-produced factors activate myeloid cells through TLR2 to stimulate metastasis. Nature *457*, 102–106.

Kuziel, W.A., Morgan, S.J., Dawson, T.C., Griffin, S., Smithies, O., Ley, K., and Maeda, N. (1997). Severe reduction in leukocyte adhesion and monocyte extravasation in mice deficient in CC chemokine receptor 2. Proc. Natl. Acad. Sci. USA *94*, 12053–12058.

Läubli, H., and Borsig, L. (2010). Selectins promote tumor metastasis. Semin. Cancer Biol. *20*, 169–177.

Läubli, H., Stevenson, J.L., Varki, A., Varki, N.M., and Borsig, L. (2006). L-selectin facilitation of metastasis involves temporal induction of Fut7-dependent ligands at sites of tumor cell arrest. Cancer Res. *66*, 1536–1542.

Läubli, H., Spanaus, K.S., and Borsig, L. (2009). Selectin-mediated activation of endothelial cells induces expression of CCL5 and promotes metastasis through recruitment of monocytes. Blood *114*, 4583–4591.

Leuschner, F., Dutta, P., Gorbatov, R., Novobrantseva, T.I., Donahoe, J.S., Courties, G., Lee, K.M., Kim, J.I., Markmann, J.F., Marinelli, B., et al. (2011). Therapeutic siRNA silencing in inflammatory monocytes in mice. Nat. Biotechnol. *29*, 1005–1010.

Loberg, R.D., Ying, C., Craig, M., Day, L.L., Sargent, E., Neeley, C., Wojno, K., Snyder, L.A., Yan, L., and Pienta, K.J. (2007). Targeting CCL2 with systemic delivery of neutralizing antibodies induces prostate cancer tumor regression in vivo. Cancer Res. *67*, 9417–9424.

Lu, X., and Kang, Y. (2009). Chemokine (C-C motif) ligand 2 engages CCR2+ stromal cells of monocytic origin to promote breast cancer metastasis to lung and bone. J. Biol. Chem. *284*, 29087–29096.

Mantovani, A., and Sica, A. (2010). Macrophages, innate immunity and cancer: balance, tolerance, and diversity. Curr. Opin. Immunol. *22*, 231–237.

McIntyre, T.M., Prescott, S.M., Weyrich, A.S., and Zimmerman, G.A. (2003). Cell-cell interactions: leukocyte-endothelial interactions. Curr. Opin. Hematol. *10*, 150–158.

Mellado, M., Rodríguez-Frade, J.M., Aragay, A., del Real, G., Martín, A.M., Vila-Coro, A.J., Serrano, A., Mayor, F., Jr., and Martínez-A, C. (1998). The chemokine monocyte chemotactic protein 1 triggers Janus kinase 2 activation and tyrosine phosphorylation of the CCR2B receptor. J. Immunol. *161*, 805–813.

Mildner, A., Mack, M., Schmidt, H., Brück, W., Djukic, M., Zabel, M.D., Hille, A., Priller, J., and Prinz, M. (2009). CCR2+Ly-6Chi monocytes are crucial for the effector phase of autoimmunity in the central nervous system. Brain *132*, 2487–2500.

Mishra, P., Banerjee, D., and Ben-Baruch, A. (2011). Chemokines at the crossroads of tumor-fibroblast interactions that promote malignancy. J. Leukoc. Biol. *89*, 31–39.

Mizutani, K., Sud, S., McGregor, N.A., Martinovski, G., Rice, B.T., Craig, M.J., Varsos, Z.S., Roca, H., and Pienta, K.J. (2009). The chemokine CCL2 increases prostate tumor growth and bone metastasis through macrophage and osteoclast recruitment. Neoplasia *11*, 1235–1242.

O'Hayre, M., Salanga, C.L., Handel, T.M., and Allen, S.J. (2008). Chemokines and cancer: migration, intracellular signalling and intercellular communication in the microenvironment. Biochem. J. *409*, 635–649.

Peinado, H., Lavotshkin, S., and Lyden, D. (2011). The secreted factors responsible for pre-metastatic niche formation: old sayings and new thoughts. Semin. Cancer Biol. *21*, 139–146.

Qian, B.Z., and Pollard, J.W. (2010). Macrophage diversity enhances tumor progression and metastasis. Cell *141*, 39–51.

Qian, B.Z., Li, J., Zhang, H., Kitamura, T., Zhang, J., Campion, L.R., Kaiser, E.A., Snyder, L.A., and Pollard, J.W. (2011). CCL2 recruits inflammatory monocytes to facilitate breast-tumour metastasis. Nature *475*, 222–225.

Reutershan, J., Morris, M.A., Burcin, T.L., Smith, D.F., Chang, D., Saprito, M.S., and Ley, K. (2006). Critical role of endothelial CXCR2 in LPS-induced neutrophil migration into the lung. J. Clin. Invest. *116*, 695–702.

Salcedo, R., Ponce, M.L., Young, H.A., Wasserman, K., Ward, J.M., Kleinman, H.K., Oppenheim, J.J., and Murphy, W.J. (2000). Human endothelial cells express CCR2 and respond to MCP-1: direct role of MCP-1 in angiogenesis and tumor progression. Blood *96*, 34–40.

Sanz-Moreno, V., Gaggioli, C., Yeo, M., Albrengues, J., Wallberg, F., Viros, A., Hooper, S., Mitter, R., Féral, C.C., Cook, M., et al. (2011). ROCK and JAK1 signaling cooperate to control actomyosin contractility in tumor cells and stroma. Cancer Cell *20*, 229–245.

Sawanobori, Y., Ueha, S., Kurachi, M., Shimaoka, T., Talmadge, J.E., Abe, J., Shono, Y., Kitabatake, M., Kakimi, K., Mukaida, N., and Matsushima, K. (2008). Chemokine-mediated rapid turnover of myeloid-derived suppressor cells in tumor-bearing mice. Blood *111*, 5457–5466.

Soria, G., Ofri-Shahak, M., Haas, I., Yaal-Hahoshen, N., Leider-Trejo, L., Leibovich-Rivkin, T., Weitzenfeld, P., Meshel, T., Shabtai, E., Gutman, M., and Ben-Baruch, A. (2011). Inflammatory mediators in breast cancer: coordinated expression of TNFα & IL-1β with CCL2 & CCL5 and effects on epithelial-to-mesenchymal transition. BMC Cancer *11*, 130.

Tremblay, P.L., Auger, F.A., and Huot, J. (2006). Regulation of transendothelial migration of colon cancer cells by E-selectin-mediated activation of p38 and ERK MAP kinases. Oncogene *25*, 6563–6573.

Yoshidome, H., Kohno, H., Shida, T., Kimura, F., Shimizu, H., Ohtsuka, M., Nakatani, Y., and Miyazaki, M. (2009). Significance of monocyte chemoattractant protein-1 in angiogenesis and survival in colorectal liver metastases. Int. J. Oncol. *34*, 923–930.

Yu, H., Pardoll, D., and Jove, R. (2009). STATs in cancer inflammation and immunity: a leading role for STAT3. Nat. Rev. Cancer *9*, 798–809.

Zhang, J., Patel, L., and Pienta, K.J. (2010). CC chemokine ligand 2 (CCL2) promotes prostate cancer tumorigenesis and metastasis. Cytokine Growth Factor Rev. *21*, 41–48.

Zijlmans, H.J., Fleuren, G.J., Baelde, H.J., Eilers, P.H., Kenter, G.G., and Gorter, A. (2006). The absence of CCL2 expression in cervical carcinoma is associated with increased survival and loss of heterozygosity at 17q11.2. J. Pathol. *208*, 507–517.